Applied Physics Letters

# Nanoimprint-assisted fabrication of high haze metal mesh electrode for solar cells

Cite as: Appl. Phys. Lett. **105**, 223901 (2014); https://doi.org/10.1063/1.4903061
Submitted: 02 October 2014 . Accepted: 15 November 2014 . Published Online: 01 December 2014

Takashi Iwahashi, Rong Yang, Noriaki Okabe, Junpei Sakurai, Jun Lin, and Daisuke Matsunaga

View Online Export Citation CrossMark

ARTICLES YOU MAY BE INTERESTED IN

Metal grid/conducting polymer hybrid transparent electrode for inverted polymer solar cells
Applied Physics Letters **96**, 203301 (2010); https://doi.org/10.1063/1.3394679

High figure-of-merit ultrathin metal transparent electrodes incorporating a conductive grid
Applied Physics Letters **96**, 041109 (2010); https://doi.org/10.1063/1.3299259

The optical and electrical properties of silver nanowire mesh films
Journal of Applied Physics **114**, 024302 (2013); https://doi.org/10.1063/1.4812390




© 2014 AIP Publishing LLC.

# Nanoimprint-assisted fabrication of high haze metal mesh electrode for solar cells

Takashi Iwahashi, Rong Yang, Noriaki Okabe, Junpei Sakurai, Jun Lin,[a)] and Daisuke Matsunaga
*Tokyo Electron Limited, 650 Mitsuzawa, Hosaka-cho, Nirasaki City, Yamanashi, Japan*

(Received 2 October 2014; accepted 15 November 2014; published online 1 December 2014)

We propose a concept of transparent electrode for solar cells surpassing conventional transparent conductive oxide. Transparent electrode requires low electrical resistivity, high optical transparency, and high optical haze. Although transparent conductive oxide by chemical vapor deposition is widely used as a transparent electrode for solar cells, a breakthrough of the trade-off between electrical and optical properties is required for further improvement of solar cell efficiency. We demonstrate solution-processed electrode fabrication by using nanoimprint technology and metal nanoparticle ink. Silver mesh electrode is self-aligned on nanoimprinted texture with concave pattern as a template for mesh grid. Our electrode concept can realize desired high optical haze by nanoimprinted texture, as well as low electrical resistivity and high optical transparency by metal mesh electrode simultaneously, which boosts solar cell efficiency. © *2014 AIP Publishing LLC*.
[http://dx.doi.org/10.1063/1.4903061]

Transparent electrode as a front contact of thin film solar cell requires three properties simultaneously which are low electrical resistivity, high optical transparency, and high optical haze. On one hand, lower resistivity reduces electrical losses and higher transparency reduces light absorption losses of solar cell. On the other hand, higher haze improves light trapping ability in the thin absorber layer, which promotes efficient light absorption in the layer. In terms of thin film silicon solar cell, light trapping ability is especially important due to thin light absorption layer.[1–3] For instance, transparent conductive oxide (TCO) deposited by chemical vapor deposition (CVD), such as F-doped tin oxide (SnO) and B-doped zinc oxide (ZnO), is widely used as a front contact of solar cell because of its intrinsic randomly-textured surface morphology which results in high optical haze.[3–5] To obtain low resistivity with CVD TCO, relatively high doping concentration is required, but this also results in low transparency because of free-carrier absorption.[6,7] Therefore, resistivity and transparency of CVD TCO suffers a trade-off relationship.

Recently, metal mesh electrodes fabricated by various techniques, such as metal nanowire and nanolithography, are attracting much interest because of its availability of lower resistivity and higher transparency relative to conventional TCO.[8,9] Such electrical and optical property of metal mesh electrode is quite suitable to display products such as flat panel display, touch panel display, and also flexible display because of its bending durability if it is coated on flexible substrate.[5,10] As for a front contact of solar cells, silver (Ag) nanowire electrode is considered to be a cost-competitive alternative to indium tin oxide (ITO) TCO widely used in solar cells because of its electrical and optical performance comparable with flat ITO.[8,11] However, existing mesh electrode concepts is not well applicable to a front contact of thin film solar cell due to its low or negligible haze resulting in poor light trapping.

Nanoimprint technology is one of the most attractive techniques in not only semiconductor but also photovoltaic fields because of its optical designability of materials.[12–14] In the semiconductor industry, nanoimprint lithography is considered to be a promising technique to realize the lithography resolution of lower than 10 nm with cheaper cost than extreme ultra-violet lithography. On the other hand, in the photovoltaic industry, nanoimprint allows us to design texture structure on the substrate surface to achieve optimal haze for efficient light trapping.[15–17] Consequently, combining of mesh electrode concept with nanoimprint technique will enable excellent transparent electrode which breaks a trade-off relationship of resistivity and transparency of TCO along with high haze.

In this study, we propose a potential concept of transparent electrode in which mesh shape and nanoimprint texture are combined. Self-aligned Ag mesh electrode is fabricated by simply coating Ag nanoparticle ink on lattice-shaped nanoimprint pattern. The potential of our nanoimprint-assisted metal mesh electrode concept was confirmed by the optical and electrical simulation based on the performance of obtained Ag mesh electrode.

Fig. 1 shows the brief nanoimprint process flow to obtain high haze mesh electrode. Mother mold with truncated square pyramid concave array was provided on silicon wafer by anisotropic dry etching with photoresist mask patterned by photolithography process as shown in Fig. 1(a). Master mold was fabricated by imprinting the mother mold to UV-cured resin on polyethylene terephthalate (PET) film as shown in Fig. 1(b). Working mold was prepared by imprinting the master mold to UV-cured resin on PET film similarly with the master mold preparation process. Finally, the glass mold with truncated square pyramid convex array was fabricated from the working mold in the same manner as the master and working molds. To obtain high haze with random texture, we deposited

[a)]Author to whom correspondence should be addressed. Electronic mail: jun.lin@tel.com

 © 2014 AIP Publishing LLC

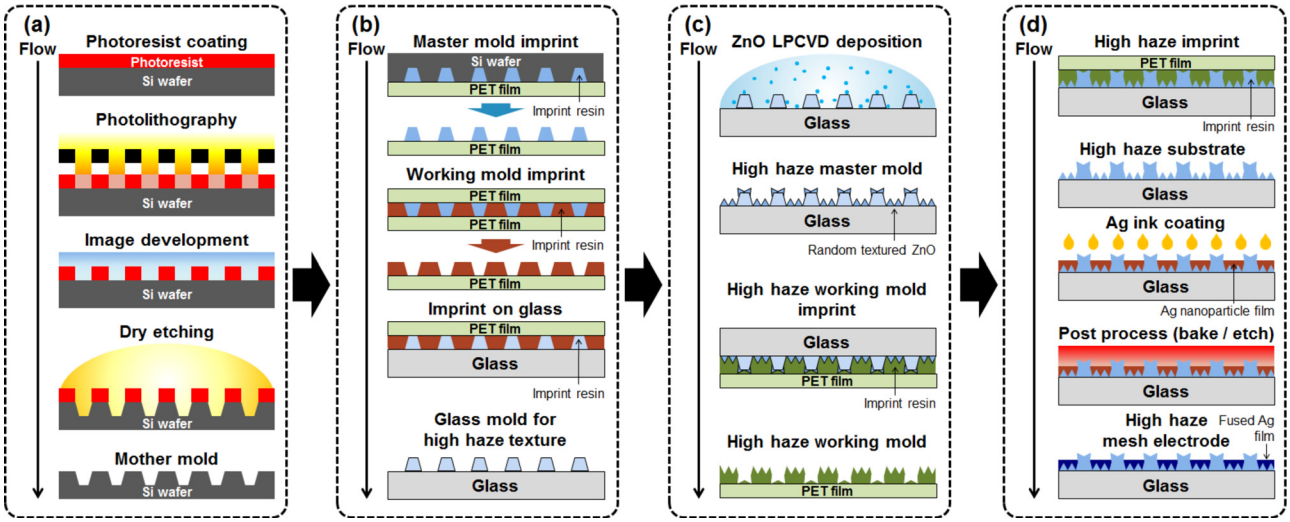


FIG. 1. Schematic image of high haze mesh electrode preparation process: (a) photolithography process flow to obtain mother mold with concave allay, (b) nanoimprint process to obtain glass mold with convex allay for high haze texture preparation, (c) LPCVD and nanoimprint process to obtain high haze working mold with concave allay, and (d) high haze nanoimprint and Ag ink coating with following post processes to achieve high haze metal mesh electrode.

ZnO on the obtained glass mold with truncated square pyramid convex array by low pressure chemical vapor deposition (LPCVD) with an industrial CVD chamber (TEL Solar AG) using di-ethyl zinc (DEZn), $H_2$, $H_2O$, and $B_2H_6$ gas mixture at a base pressure of 50 Pa at 190 °C as shown in Fig. 1(c). The target thickness of ZnO was 1.0 $\mu$m. We used the obtained glass mold as a high haze master mold to fabricate the high haze working mold which imprints truncated square pyramid convex array with random-texture on the glass substrate.

Brief image of Ag mesh electrode preparation process with obtained high haze working mold is shown in Fig. 1(d). High haze texture was imprinted on the glass substrate by using UV-cured resin with the obtained high haze working mold in the same manner as the glass mold mentioned above. Ag nanoparticle ink was provided by dispersing commercial Ag nanoparticle (Sigma-Aldrich) with its size of $\leq$50 nm into ethanol. Obtained Ag nanoparticle ink was spin-coated on the textured glass substrate to obtain the Ag mesh electrode. Ag nanoparticles precipitate preferentially in V-shaped concave grid pattern, and therefore, Ag mesh grid is aligned automatically. The obtained Ag mesh electrode was annealed at 270 °C to reduce resistivity of Ag mesh grid by fusing Ag nanoparticles. Finally, wet etching process with diluted nitric acid aqueous solution was performed to remove Ag nanoparticle precipitates on the region other than V-shaped concave. Such Ag nanoparticles are relatively well isolated although Ag nanoparticles in V-shaped concave are linked and sustained each other, so we can selectively remove such isolated Ag nanoparticles at the area other than V-shaped concave by wet etching process.

Figs. 2(a) and 2(b) show the SEM images of the glass mold with the truncated square pyramid convex array and

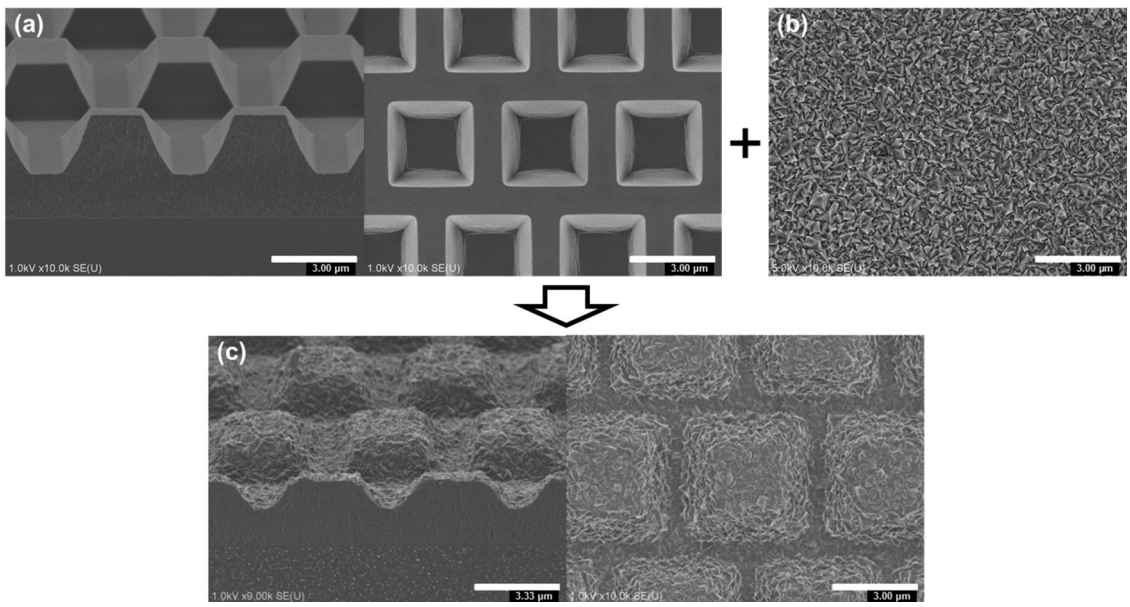


FIG. 2. SEM images of (a) glass mold with truncated square pyramid convex array, (b) LPCVD ZnO with random-texture on flat substrate and (c) imprinted high haze glass substrate in which convex array and randam-texture are combined. The magnification ratio is set to be 9000× or 10 000×.

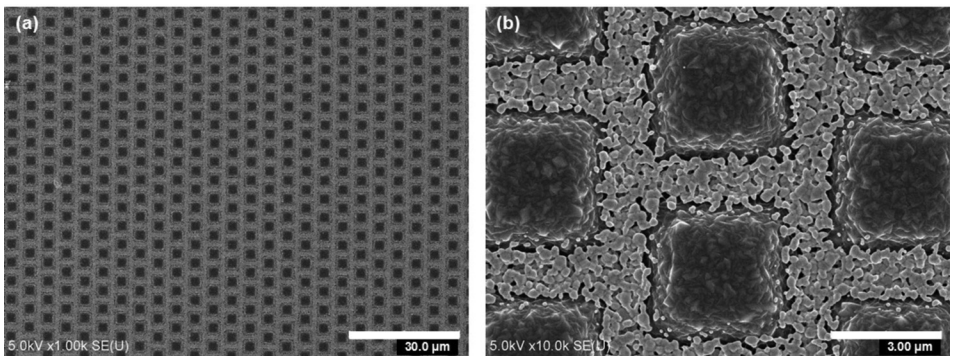


FIG. 3. SEM images of obtained Ag mesh electrode with the magnification ratio of (a) 1000× and (b) 10 000×. Uniform Ag mesh grid pattern is obtained.

the LPCVD ZnO random-texture on the flat glass substrate. The resulting texture structure with combination of the truncated square pyramid convex array and the random-texture is shown in Fig. 2(c), which includes V-shaped concave grid pattern as a template of metal mesh electrode. Fig. 3 shows the obtained Ag mesh electrode by the entire process mentioned above, and we found that Ag nanoparticles selectively aggregate in the V-shaped convex grid and are fused to each other. This result clearly indicates that metal mesh electrode is fabricated with our simple approach.

Next, we performed sheet resistance, transmittance, and haze measurements to confirm the electrical and optical performance of obtained Ag mesh electrode. Same measurement is also performed for the conventional CVD TCO to compare the performance. Here, B-doped ZnO (BZO) deposited by LPCVD process is chosen as a representative CVD TCO. Fig. 4 summarizes the comparison of the electrical and optical properties for the BZO and the Ag mesh electrode fabricated in this study. Transmittance and haze given in Fig. 4 are the averaged values in the spectral region from 400 nm to 1100 nm of obtained transmittance and haze spectra of each electrode. Here, we define transmittance as 100% for bare substrate without electrode layer such as BZO and Ag mesh. As is clearly seen in Fig. 5, the Ag mesh electrode exhibits lower sheet resistance with higher haze simultaneously relative to BZO. On the other hand, transmittance of Ag mesh electrode is slightly lower than that of BZO. This is attributed to relatively large coverage of Ag mesh electrode area due to wide V-shaped concave grid pattern width as shown in Fig. 3(b).

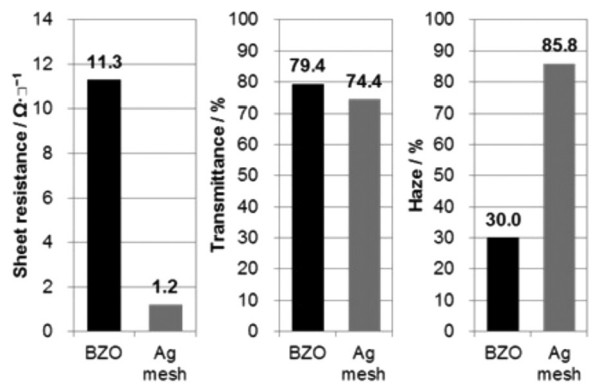


FIG. 4. Comparison of electrical and optical properties of (left) sheet resistance (center) transmittance and (right) haze for representative conventional TCO of BZO and obtained Ag mesh electrode.

To confirm the potential of our Ag mesh electrode concept, the electrode coverage dependence of sheet resistance and transmittance is simulated from the measured sheet resistance, transmittance, and electrode coverage of the mesh electrode sample fabricated in this study. The electrode coverage is estimated to be 54% from the SEM image of Fig. 3(b). Fig. 5 shows the simulation result obtained by assuming constant electrode thickness for all the coverage range. Transmittance is not zero even with the coverage of 100%, and this is because the obtained Ag mesh electrode is relatively porous and thin, which is confirmed by cross-section SEM (not shown) to be less than a few hundred nm. The trade-off between sheet resistance and transmittance of TCO is difficult to improve, and conventional BZO, for example, has a sheet resistance higher than 10 Ω/□ at a given transmittance of 90%. However, as is clearly seen in Fig. 5, the simulation result indicates the presence of the optimal coverage range at the shadowed area where lower sheet resistance and higher transmittance can be achieved simultaneously beyond the trade-off relationship of conventional TCO. This result strongly suggests that our Ag mesh electrode concept can realize higher electrical and optical properties simultaneously than the limitation of conventional TCO by adjusting the electrode coverage in the range from 7% (transmittance can be improved up to 95% while keeping sheet resistance of 10 Ω/□) to 21% (sheet resistance can be reduced to 3 Ω/□ while keeping transmittance of 90%). The electrode coverage can be controlled by changing V-shaped concave grid

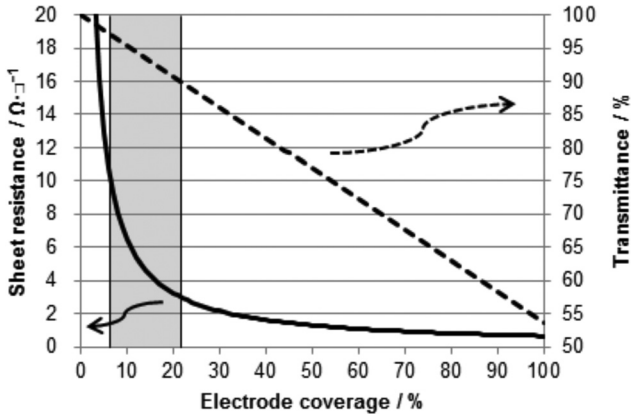


FIG. 5. Simulated electrode coverage dependence of sheet resistance (solid line) and transmittance (dashed line) for Ag mesh electrode. The coverage range at the shadowed area possesses lower resistance and higher transmittance simultaneously beyond the trade-off relationship of the conventional TCO.

pattern width of nanoimprint template, which is achievable by changing the line width of the photomask pattern used in the photolithography process of mother mold preparation in Fig. 1(a).

It is also noticeable that the simulation result shown in Fig. 5 is based on the constant electrode thickness as mentioned above. This means that much lower sheet resistance without lowering transmittance is achievable with thicker Ag mesh electrode line, which can be assembled by deeper V-shaped concave grid pattern with the same grid line width. Such texture shape with higher aspect ratio can be obtained by controlling the dry etching process of mother mold preparation in Fig. 1(a). If we consider 5 times thicker electrode line with the controlled coverage of 5% based on the simulation result in Fig. 5 for example, we will obtain an Ag mesh grid with in roughly the sheet resistance of $<3\ \Omega/\square$ and the transmittance of $>95\%$, which is far beyond the trade-off relationship of conventional TCO. Thus, we can conclude that our Ag mesh electrode concept possesses a great possibility to be a breakthrough of the trade-off relationship of the current transparent electrode performance for solar cell technology.

In summary, we demonstrated a concept of transparent electrode in which mesh shape and nanoimprint texture are combined. V-shaped concave grid pattern as a template of mesh electrode is fabricated on the glass substrate by arraying truncated square pyramid with ZnO-type random texture with use of nanoimprint technique based on a film mold imprinting method. Ag mesh electrode is fully self-aligned by simply coating Ag nanoparticle ink and sequential anneal and wet etch processes. Obtained Ag mesh electrode with transparency comparable to conventional TCO exhibits higher haze and lower sheet resistance. The simulation based on the electrical and optical properties of obtained Ag mesh electrode clearly indicates that the optimized electrode coverage and thickness, which can be obtained by controlling nanoimprint template shape with optimal mother mold preparation process, gives highly balanced electrical and optical performance surpassing the conventional TCO potential. We have already demonstrated previously the nanoimprint technique which realizes highly flexible structure design with scalability.[18,19] The lithography for mother mold fabrication is expensive; however, for our nanoimprint technology, the same mother mold can be used for many times to replicate the texture on glass, which reduces the cost dramatically and is possible to meet the cost requirement of manufacturing. Consequently, we conclude that optimization of metal grid template will realize more balanced transparent electrode with low resistivity, high transparency, and desired haze boosting thin film solar cell efficiency.

[1]D. Dominé, P. Buehlmann, J. Bailat, A. Billet, A. Feltrin, and C. Ballif, Phys. Status Solidi (RRL) **2**, 163 (2008).
[2]Y. Nasuno, N. Kohama, K. Nishimura, T. Hayakawa, H. Taniguchi, and M. Shimizu, Appl. Phys. Lett. **88**, 071909 (2006).
[3]T. Söderström, F.-D. Haug, V. Terrazzoni-Daudrix, and C. Ballif, J. Appl. Phys. **103**, 114509 (2008).
[4]K. Sato, Y. Gotoh, Y. Wakayama, Y. Hayashi, K. Adachi, and H. Nishimura, Rep. Res. Lab. Asahi Glass Co., Ltd. **42**, 129 (1992).
[5]X. Fan, F. Wang, Z. Chu, L. Chen, C. Zhang, and D. Zou, Appl. Phys. Lett. **90**, 073501 (2007).
[6]W. W. Wenas, A. Yamada, K. Takahashi, M. Yoshino, and M. Konagai, J. Appl. Phys. **70**, 7119 (1991).
[7]S. Faÿ, J. Steinhauser, N. Oliveira, E. Vallat-Sauvain, and C. Ballif, Thin Sol. Films. **515**, 8558 (2007).
[8]J.-Y. Lee, S. T. Connor, Y. Cui, and P. Peumans, Nano Lett. **8**, 689 (2008).
[9]M.-G. Kang, H. J. Park, S. H. Ahn, and L. J. Guo, Sol. Energy Mater. Sol. Cells. **94**, 1179 (2010).
[10]X. Huang, P. Shen, B. Zhao, X. Feng, S. Jiang, H. Chen, H. Li, and S. Tan, Sol. Energy Mater. Sol. Cells. **94**, 1005 (2010).
[11]R. Zhu, C.-H. Chung, K. C. Cha, W. Yang, Y. B. Zheng, H. Zhou, T.-B. Song, C.-C. Chen, P. S. Weiss, G. Li, and Y. Yang, ACS Nano **5**, 9877 (2011).
[12]L. J. Guo, J. Phys. D: Appl. Phys. **37**, R123 (2004).
[13]H. Schift, J. Vac. Sci. Technol. B. **26**, 458 (2008).
[14]J. J. Dumond and H. Y. Low, J. Vac. Sci. Technol. B. **30**, 010801 (2012).
[15]C. Battaglia, K. Söderström, J. Escarré, F.-J. Haug, D. Dominé, P. Cuony, M. Boccard, G. Bugnon, C. Denizot, M. Despeisse, A. Feltrin, and C. Ballif, Appl. Phys. Lett. **96**, 213504 (2010).
[16]K. Söderström, J. Escarré, O. Cubero, F.-J. Haug, S. Perregaux, and C. Ballif, Prog. Photovoltaics **19**, 202 (2011).
[17]C. Battaglia, J. Escarré, K. Söderström, L. Erni, L. Ding, G. Bugnon, A. Billet, M. Boccard, L. Barraud, S. D. Wolf, F.-J. Huag, M. Despeisse, and C. Ballif, Nano Lett. **11**, 661 (2011).
[18]J. Lin, H. Yoshida, T. Iwahashi, T. Harada, J. Sakurai, T. Fujibayashi, A. Tsuji, J. Hoetzel, J.-B. Orhan, M. Hannu-Kuure *et al.*, *Proceedings of the 28th European Photovoltaic Solar Energy Conference, Paris, France* (WIP, 2013), pp. 2152–2154.
[19]J. Lin, J. Cashmore, T. Iwahashi, J. Sakurai, P. Losio, J.-B. Orhan, J. Hoetzel, S. Ristau, Y. Saito, A. Tsuji *et al.*, Proceedings of the 40th IEEE Photovoltaic Specialist Conference, Denver, USA, 2014 (unpublished).